Inorganic Chemistry

ARTICLE

pubs.acs.org/IC

Deciphering Three Beneficial Effects of 2,2′-Bipyridine-*N*,*N*′-Dioxide on the Luminescence Sensitization of Lanthanide(III) Hexafluoroacetylacetonate Ternary Complexes

Svetlana V. Eliseeva,*[,†,‡] Dmitry N. Pleshkov,[†] Konstantin A. Lyssenko,[§] Leonid S. Lepnev,[∥] Jean-Claude G. Bünzli,[‡] and Natalia P. Kuzmina[†]

[†]Laboratory of Chemistry of Coordination Compounds, Lomonosov Moscow State University, 1-3 Leninskie Gory, 119991 Moscow, Russia

[‡]Institute of Chemical Sciences and Engineering, Swiss Federal Institute of Technology Lausanne (EPFL), BCH 1403, CH-1015 Lausanne, Switzerland

[§]A. N. Nesmeyanov Institute of Organoelement Compounds, Russian Academy of Sciences, 28 Vavilov Street, 119991 Moscow, Russia

[∥]Lebedev Physical Institute, Russian Academy of Sciences, Optics, 53 Leninsky Prosp., 119991 Moscow, Russia

Supporting Information

ABSTRACT: Lanthanide hexafluoroacetylacetonate ternary complexes with 2,2′-bipyridine-*N*,*N*′-dioxide, $[Ln(hfa)_3(bpyO2)]$, were synthesized for Ln = Eu, Gd, Tb, and Lu and fully characterized by elemental, thermal, and mass-spectrometric analyses. The X-ray crystal structure of $[Eu(hfa)_3(bpyO2)]\cdot 0.5C_6H_6$ reveals an octa-coordinate metal ion lying in a severely distorted trigonal dodecahedron geometry; the Eu−O distances lie in the range 2.36−2.44 Å with no significant difference between hfa^- and bpyO2. A detailed comparative photophysical investigation has been carried out to determine the exact influence of the introduction of bpyO2 in the inner coordination sphere of the metal ion in replacement of the two water molecules in $[Ln(hfa)_3(H_2O)_2]$. While this replacement is detrimental for Tb, it leads to a 15-fold increase in the overall quantum yield for Eu. This large improvement originates from (i) a better sensitization efficiency, the ancillary ligand being responsible for 3/4 of the energy transfer, (ii) elimination of nonradiative deactivation pathways through harmonics of O−H vibrations, and (iii) reduction in the radiative lifetime. The latter influence is rarely documented, but it accounts here for a ≈25% increase in the intrinsic quantum yield, so that more attention should be given to this parameter when designing highly luminescent lanthanide complexes.

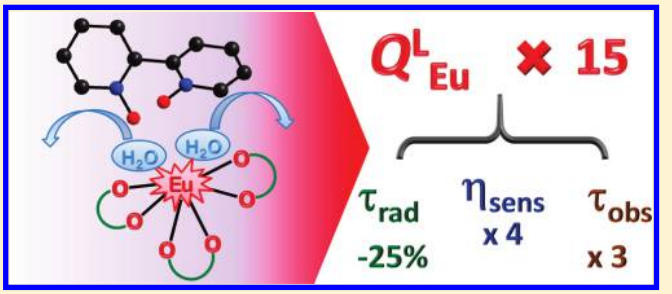

INTRODUCTION

Lanthanide β-diketonates are among the best studied rare-earth luminescent complexes[1] because they are brightly emissive[2] and volatile,[3] which makes them valuable precursors for electroluminescent layers.[4] In addition, their photophysical properties can be tuned almost at will by a judicious choice of ancillary ligands.[5−8] Indeed, conventional synthesis usually yields bis(hydrated) tris(β-diketonates), but the two solvent molecules can be effortlessly substituted by either a fourth diketonate anion or a bidentate donor ligand which may be functionalized so as to provide convenient light-harvesting and subsequent energy transfer onto the metal ion. Lanthanide β-diketonates and their derivatives are amenable to incorporation into all kind of materials, from thin films,[9] to ionic liquids,[10] mesoporous[11] or microporous[12] hybrids, and nanoparticles.[13] The unmatched luminescent properties of β-diketonate compounds and materials are at the heart of a number of applications, ranging from analytical sensors,[14−16] emissive layers for organic light-emitting diodes (OLEDs),[17−19] including white-light production,[20,21] nonlinear optics,[22] as well as time-resolved bioanalyses[23] and bioimaging.[24,25] It is noteworthy that not only visible but also near-infrared luminescence[26,27] is efficiently sensitized in β-diketonate ternary complexes.

When examining photophysical parameters reported in the literature for water-free β-diketonates, one realizes that at first sight data may seem to be contradictory in the sense that irrespective of large quantum yields, up to 85% for Eu^{III},[28] lifetimes of the excited states remain short, in spite of little vibrational quenching in the first coordination sphere. Typical values for $Eu(^5D_0)$ are in the range 0.3−0.7 ms whereas much longer lifetimes are reported for other classes of compounds with similar quantum yields (1.5−2.5 ms). This is most probably due to β-diketonates inducing appreciable admixture of ligand orbitals into 4f wave functions, henceforth leading to relatively short radiative lifetimes.[29] In this way, the Laporte's forbidden f-f transitions become more probable, and the observed lifetimes are comparatively short. Generally speaking, replacing the two

Received: March 5, 2011
Published: May 05, 2011

Table 1. Selected Structural Parameters for $[Eu(hfa)_3(bpyO2)]\cdot 0.5C_6H_6$[a]

	Eu−O/ Å		O−Eu−O/ deg
		hfa$^-$	
a	2.3609(15)	2.4430(15)	71.14(5)
b	2.3851(15)	2.3900(15)	73.15(5)
c	2.3852(15)	2.4033(16)	72.78(6)
		2.395(27)	***72(1)***
		(bpyO2)	
	2.3775(14)		71.43(5)
	2.3661(15)		
	2.372(8)		

[a] Data in bold italic are average values; standard deviations are given between parentheses.

water molecules in the inner coordination sphere of tris(β-diketonates) is expected to have two beneficial effects: (i) the removal of O−H induced vibrational quenching and (ii) depending on the electronic levels of the ancillary ligands, enhancement of the energy transfer processes resulting in luminescence sensitization.[30,31] These two effects are repeatedly mentioned in the literature but rarely quantified separately. In addition, to our knowledge, there is no mention of the potential effect of the ancillary ligand on the radiative lifetime of the excited Ln^{III} level.

In this work, we aim at quantitatively elucidating the beneficial effects of 2,2′-bipyridine-*N*,*N*′-dioxide (bpyO2) as ancillary ligand on the photophysical properties of $[Ln(hfa)_3(bpyO2)]$ (Ln = Eu, Tb). We have selected this ligand because 2,2′-bipyridine-*N*,*N*′-dioxide is an efficient chromophore for the sensitization of lanthanide luminescence either as such,[32,33] or when grafted onto podands[34] or calix[4]arenes.[35] Indeed, the preferred binding of Ln^{III} ions, which are hard Lewis acids, to oxygen-donor ligands make them ideal for the design of efficient luminescent materials because high bond-valence contribution of the *O*-donors leads to more 4f orbital mixing and thus to luminescence enhancement. Here, a detailed analysis of the relevant sensitization parameters for Ln = Eu allows us to decipher the role of the ancillary ligand with respect to vibrational quenching removal, contribution to energy transfer, and radiative lifetime shortening resulting in the large luminescence enhancement observed when going from $[Ln(hfa)_3(H_2O)_2]$ to the ternary complex.

RESULTS AND DISCUSSION

Synthesis and Characterization. The reaction of 2,2′-bipyridine-*N*,*N*′-dioxide (bpyO2) with equimolar amounts of $[Ln(hfa)_3(H_2O)_2]$ (Ln^{III} = Eu, Gd, Tb, Lu) under reflux in benzene or toluene results in the formation of air-stable complexes with general composition $[Ln(hfa)_3(bpyO2)]$ which were isolated by decantation as colorless precipitates upon cooling the solution to room temperature. The isolated complexes were characterized by elemental analysis, IR spectroscopy and in case of Eu^{III} compounds by LDI-TOF mass-spectrometry in view of their easy-to-recognize isotopic distribution.

IR spectra of $[Ln(hfa)_3(bpyO2)]$ are similar for all lanthanide ions studied and present bands in the range 1650−1430 cm^{-1} assigned to C═O and C═C vibrations of the chelate ring, typical of fluorinated β-diketonates, as well as of the breathing modes of the pyridine ring of ancillary ligand. Characteristic C−H vibrations appear in the range 3000−3200 cm^{-1}. The assignment of bands in the 1100−1300 cm^{-1} spectral range is difficult because of overlap of ν(C−F) of hfa^- and ν(N−O) of bpyO2. Absence of broad-band absorption at 3200−3500 cm^{-1} confirms that all $[Ln(hfa)_3(bpyO2)]$ are devoid of water molecules.

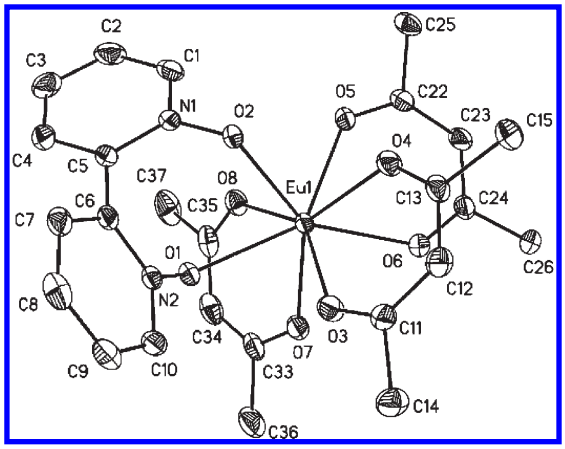

Figure 1. Molecular structure of $[Eu(hfa)_3(bpyO2)]\cdot 0.5C_6H_6$ (**1**) (50% probability ellipsoids, F and H atoms as well as solvate benzene molecules are omitted for clarity).

Crystal and Molecular Structure of the Eu^{III} Complex. Single crystals of $[Eu(hfa)_3(bpyO2)]\cdot 0.5C_6H_6$ (**1**) of satisfying quality could be obtained by slow evaporation of the corresponding ternary complex in benzene. X-ray diffraction analysis revealed this compound crystallizing in the monoclinic space group $P2_1/n$ and being mononuclear. Corresponding selected structural parameters are listed in Table 1.

The Eu^{III} ions are well separated in the crystal structure, with Eu···Eu distances larger than 9.6 Å, an asset for efficient luminescence since energy migration between metal ions will be minimized. The metal ions are surrounded by eight oxygen atoms, six of them provided by anionic β-diketone ligands and two by the bpyO2 ancillary ligand acting as a bidentate chelating agent (Figure 1). The hfa^- anions are coordinated differently: while $hfa(b)^-$ and, to a lesser extent, $hfa(c)^-$ are almost symmetrically bound (Δ(Eu−O) < 0.015 Å), $hfa(a)^-$ displays two Eu−O distances which differ by 0.08 Å, and its bite angle is slightly smaller, ≈ 71° versus ≈73° for the other two anions. Such asymmetry in the Eu−O(hfa) bond lengths is quite typical for lanthanide β-diketonates and might be caused by weak intermolecular interactions leading to highest-density packing in the crystal structure.[36,37] Altogether, the Eu−O(hfa) distances vary from 2.3609(15) to 2.4430(15) Å with an overall average value of 2.395 Å. They lie within the range observed for other ternary complexes containing hfa^-: for instance, 2.38(3) Å for the recently reported coordination polymers $[Eu(hfa)_3(Q)]_\infty$ (Q = 1,4-diacetylbenzene, 1,4-diacetoxybenzene, or 1,4-dimethyltherephtalate)[6] or 2.43(5) Å for $[Eu(hfa)_3(bpy)(H_2O)]\cdot$ bpy (bpy = 2,2′-bipyridine).[38]

The bpyO2 ligand is almost symmetrically coordinated, with a mean Eu−O(bpyO2) bond length of 2.372 Å, which is similar to the one observed for the europium chloride complex, $[EuCl_3(bpyO2)]\cdot 2CH_3OH$, 2.38 Å,[39] but somewhat shorter than in $[Eu(bpyO2)_4][ClO_4]_3$, 2.40 Å.[33] Interestingly, the mean Eu−O(bpyO2) bond length is very close to the average of the five shortest Eu−O(hfa) distances, 2.38(2) Å while its bite angle is similar to the one of $hfa(a)^-$.

dx.doi.org/10.1021/ic200450x |*Inorg. Chem.* 2011, 50, 5137–5144

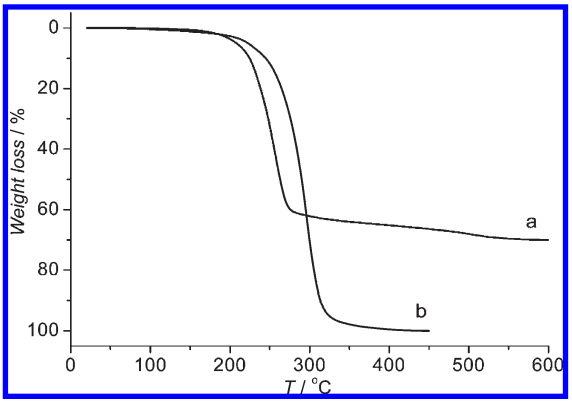

Figure 2. Weight loss of $[Gd(hfa)_3(bpyO2)]$ versus temperature: (a) under nitrogen atmosphere and (b) under vacuum.

The repulsion between oxygen and, to a lesser extent, hydrogen atoms in the ancillary ligand leads to rotation of the pyridine rings around the C5−C6 bond. The torsion angle N1−C5−C6−N2 in **1** is equal to 62.6°, the same as the average value in $[Nd(bpyO2)_4][ClO_4]_3$,[32] but smaller than that in the free bpyO2 ligand, 70.9°.[40] This rotation can also be characterized by another parameter, the degree of bending (DB),[41] defined as the sum of angles between the C−C bond and the pyridine rings; the DB increases in going from the free ancillary ligand, 1.4°,[40] to the bound ligand in **1**, 7.2°. As a comparison, the DB of the bpyO2 ligands in the homoleptic complex $[Nd(bpyO2)_4][ClO_4]_3$ ranges from 2.8 to 5.6°,with a mean value of 4.4°.[32]

The relative bonding strengths of the ligands were quantified by the bond-valence contribution, $\nu_{Ln,j}$, using the bond-valence method.[42,43] The average $\nu_{Ln,j}$(hfa) value is equal to 0.38(3), while that of bpyO2 is marginally larger, 0.40(1), in line with expectations based on the ligand charges but at variance with the mean values of Eu−O(hfa) and Eu−O(bpyO2) (Table 1, discussion above). The calculated bond-valence sum V_{Ln} is 3.09 and matches well the formal oxidation state of Eu^{III} ion (+3.00) within the accuracy of the method (±0.25 valence units).

To get more insights into the coordination geometry around Eu^{III} ion and estimate the degree of distortion from ideal 8-coordination polyhedra, the "shape measure" criterion *S*, suggested by Raymond et al.,[44] was estimated as follows:

$$S = \min \sqrt{((1/m)\sum_{i=1}^{m}(\delta_i - \theta_i)^2)} \qquad (1)$$

here *m* is the number of all possible edges, δ_i is the observed dihedral angle along the *i*th edge of the experimental polyhedron δ, and θ_i is the same angle for the corresponding ideal polytopic shape θ. The three most commonly encountered 8-coordination polyhedra were considered: the square antiprism (SAP, D_{4d}), the trigonal dodecahedron (DOD, D_{2d}), and the bicapped trigonal prism (BCTP, C_{2v}).[45] Analysis of the data shows that the coordination polyhedron around the Eu^{III} ion deviates substantially from an ideal polyhedron and is best described as a distorted trigonal dodecahedron:

$$S(D_{4d}) = 14.12, \quad S(D_{2d}) = 10.13, \quad S(C_{2v}) = 11.04$$

Thermal Analysis. Since thermal behavior, particular stability and volatility, is important for practical applications in electroluminescent materials, $[Ln(hfa)_3(bpyO2)]$ (Ln^{III} = Eu−Tb) were investigated by means of thermal analysis under nitrogen atmosphere and in vacuum. In general, the thermal behavior of the reported complexes was independent of the nature of the lanthanide ion; therefore, the following discussion is restricted to Gd^{III} complexes only.

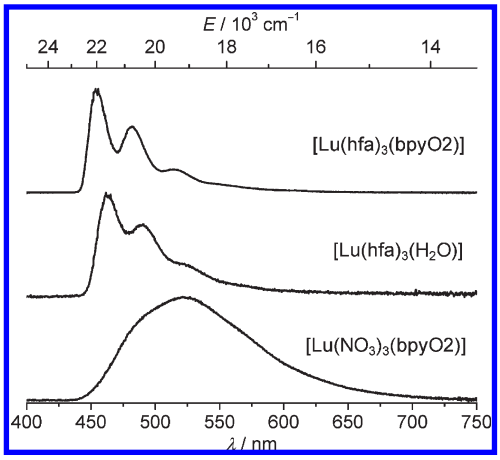

Figure 3. Phosphorescence spectra of Lu^{III} complexes in solid state under excitation at 337 nm; *T* = 77 K.

No weight loss is observed up to 190 °C both under nitrogen and in vacuum (Figure 2). Upon further heating, the thermal behavior of $[Gd(hfa)_3(bpyO2)]$ is different depending on the atmosphere. Under nitrogen, weight loss occurs in two steps but decomposition does not reach completion even at 600 °C: the total weight loss (70%) is lower than the one corresponding to transformation into fluoride (78%), oxyfluoride (80%), oxide (81%), or their mixtures. In vacuum, on the other hand, the total weight loss for $[Gd(hfa)_3(bpyO2)]$ reaches 100%, which can be attributed to substantial sublimation of the complex. So, thermal deposition of thin films of $[Ln(hfa)_3(bpyO2)]$ can be envisaged in vacuum. Detailed investigation of the thermal behavior of $[Ln(hfa)_3(bpyO2)]$ is presently under way to prove the probability of intact sublimation.

Photophysical Properties. *Ligand-Centered Luminescence.* It is commonly accepted that one of the major channel for energy transfer in lanthanide coordination compounds involves long-lived triplet states of organic ligands.[46] Therefore, it becomes an important issue to determine the energy of the triplet state, $E_{T(0-0)}$. Usually, Gd^{III} compounds are optimum for this purpose, because of their structural similarity with Eu^{III} and Tb^{III} complexes on one hand, and, on the other hand, the larger probability of ligand phosphorescence because of combination of both paramagnetic[47] and heavy-atom[48] effects. In addition, the $^6P_{7/2}$ state of Gd^{III} ion lies at too high energy to be populated through most organic ligands. However, in our case, it became a real problem to obtain phosphorescence spectra of either $[Gd(NO_3)_3(bpyO2)]$ or $[Gd(hfa)_3(bpyO2)]$ because even when high purity Gd_2O_3 oxide (99.998%) was used as a starting reagent, minute amounts of Eu^{III} in it led to almost complete quenching of the phosphorescence emission. We therefore moved to Lu^{III} complexes, which were successfully synthesized and their phosphorescence spectra were measured and compared with the one of the starting material $[Lu(hfa)_3(H_2O)_2]$ (Figure 3). The $E_{T(0-0)}$ energy of the bpyO2 ligand was estimated from Gaussian decomposition of the broad-band $[Lu(NO_3)_3(bpyO2)]$ spectrum centered at ~525 nm and found to be 20 540 cm^{-1}. The general envelope of the phosphorescence spectrum of the ternary

dx.doi.org/10.1021/ic200450x |*Inorg. Chem.* 2011, 50, 5137–5144

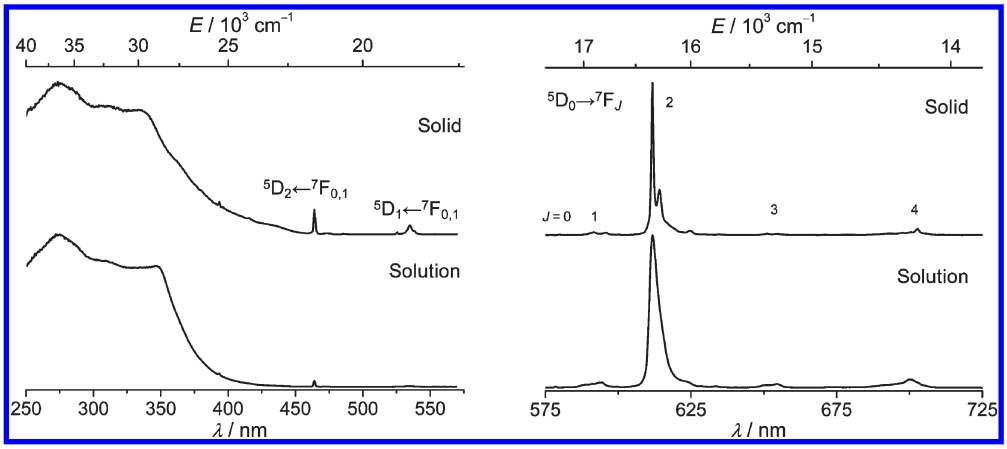

Figure 4. (Left) Excitation ($^5D_0 \rightarrow {}^7F_2$ transition) and (right) emission (λ_{ex} = 340 nm) spectra of [Eu(hfa)$_3$(bpyO2)] in the solid state and solution 1 mM in CH_2Cl_2 at 295 K.

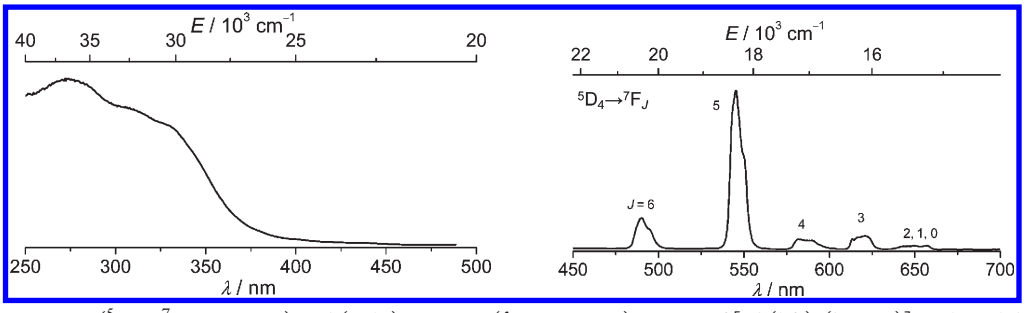

Figure 5. (Left) Excitation ($^5D_4 \rightarrow {}^7F_5$ transition) and (right) emission (λ_{ex} = 340 nm) spectra of [Tb(hfa)$_3$(bpyO2)] in the solid state at 295 K.

complex [Lu(hfa)$_3$(bpyO2)] is very similar to the one of [Lu(hfa)$_3$-(H$_2$O)$_2$], with only a slight blue shift of about 10 cm^{-1}. It presents three distinct bands at 455 (21 980 cm^{-1}), 480 (20 830 cm^{-1}), and 515 (19 420 cm^{-1}) nm, that is, it resembles the superposition of the phosphorescence spectra of the two organic ligands. Therefore, in ternary complexes a path for energy transfer may originate from the triplet states of both hfa$^-$ and bpyO2. If one considers the energy gaps between $^5D_0$ (Eu^{III}) and $^5D_4$ (Tb^{III}) and compares them with optimum values,[49] one can predict that Eu^{III} characteristic emission in [Ln(hfa)$_3$(bpyO2)] will be efficiently sensitized, ($E_{T(0-0)}$(bpyO2)$-{}^5D_0$) = 3240 cm^{-1}, while in the case of Tb^{III}, ($E_{T(0-0)}$(bpyO2)$-{}^5D_4$) = 40 cm^{-1}, back energy transfer will probably play a crucial and detrimental role.

Metal-Centered Luminescence. Excitation spectra of [Ln(hfa)$_3$(bpyO2)] (Ln = Eu, Tb) present broad bands in the range 250−450 nm with faint f-f transitions at 394 nm (25 380 cm^{-1}, $^5L_6 \leftarrow {}^7F_{0,1}$), 464 nm (27 475 cm^{-1}, $^5D_2 \leftarrow {}^7F_{0,1}$), and 535 nm (18 690 cm^{-1}, $^5D_1 \leftarrow {}^7F_{0,1}$) in case of Eu^{III} compounds, thus confirming the better sensitization of metal-centered luminescence through ligand states. Indeed, under excitation at 337 nm, both [Eu(hfa)$_3$(bpyO2)] and [Tb(hfa)$_3$(bpyO2)] display only the characteristic red and green luminescence due to $^5D_0 \rightarrow {}^7F_J$ (J = 0−4) or $^5D_4 \rightarrow {}^7F_J$ (J = 6−0) transitions, respectively (Figures 4, 5).

The Eu^{III} emission spectrum is sharp in the case of the solid state sample but becomes broader for the solution in CH_2Cl_2 (Figure 4), however, without pronounced change in the distribution of integral intensities between $^5D_0 \rightarrow {}^7F_J$ transitions (Table 2). They are dominated by the hypersensitive $^5D_0 \rightarrow {}^7F_2$ transition which represents 83−84% of the total integral intensity, an evident advantage for the design of monochromatic emitters. The highly forbidden $^5D_0 \rightarrow {}^7F_0$ transition, according to selection rules on S, L, and J quantum numbers, is measurable, although faint since it represents less than 0.1% of the total integral intensity, in line with the previous discussion about the distortion of the coordination geometry around the Eu^{III} ion in [Eu(hfa)$_3$(bpyO2)] from the ideal D_{2d} trigonal dodecahedron, for which symmetry-related selection rules additionally forbid this transition.[50]

Table 2. Integral Intensities[a] of $^5D_0 \rightarrow {}^7F_J$ (J = 0−4) and $^5D_4 \rightarrow {}^7F_J$ (J = 6−0) Transitions for Eu^{III} and Tb^{III} Complexes, Respectively

compound	state	$\int_{0-0}$	$\int_{0-1}$	$\int_{0-2}$	$\int_{0-3}$	$\int_{0-4}$	$\int_{tot}/\int_{0-1}$
[Eu(hfa)$_3$(H$_2$O)$_2$]	solid	0.17	1.00	14.3	0.38	1.72	17.6
[Eu(hfa)$_3$(bpyO2)]	solid	0.02	1.00	19.8	0.47	2.50	23.8
	solution[b]	0.02	1.00	21.1	0.63	2.31	25.0
	thin film[c]	0.02	1.00	14.6	0.54	2.19	18.3
compound	state	$\int_{4-6}$	$\int_{4-5}$	$\int_{4-4}$	$\int_{4-3}$	$\int_{4-2,1,0}$	
[Tb(hfa)$_3$(H$_2$O)$_2$]	solid	0.22	1.00	0.11	0.08	0.04	
[Tb(hfa)$_3$(bpyO2)]	solid	0.22	1.00	0.11	0.11	0.04	

[a] Experimental error, ± 5%. [b] c = 1 mM in CH_2Cl_2. [c] Obtained by thermal evaporation in vacuum ($P < 3 \times 10^{-5}$ Torr) at 200−250 °C.

In general, all photophysical parameters for [Eu(hfa)$_3$-(bpyO2)] show significant improvement over the parent hydrate [Eu(hfa)$_3$(H$_2$O)$_2$] (Table 3). The luminescence lifetime of

dx.doi.org/10.1021/ic200450x |Inorg. Chem. 2011, 50, 5137–5144

Table 3. Photophysical Parameters of Eu^{III} and Tb^{III} Complexes under Ligand Excitation (340 nm)[a]

compound	solvent	τ_{obs}, ms 295 K	τ_{obs}, ms 77 K	τ_{rad}, ms[b]	Q^{Eu}_{Eu}, %[b]	Q^{L}_{Ln}, %	η_{sens}, %[b]
$[Eu(hfa)_3(H_2O)_2]$[c]	solid	0.22(1)	0.32(1)	1.13	19	2.6	13
$[Eu(hfa)_3(bpyO2)]$	solid	0.70(1)	0.67(1)	0.85	82	40(1)	49
	CH_2Cl_2	0.60(1)	n.a.	0.94	64	35(1)	55
$[Tb(hfa)_3(H_2O)_2]$[c]	solid	0.53(1)	0.72(1)	n.a.	n.a.	27	n.a.
$[Tb(hfa)_3(bpyO2)]$	solid	$<5 \times 10^{-5}$	0.69(1)	n.a.	n.a.	0.75(6)	n.a.

[a] Data for 295 K unless otherwise stated. Standard deviation (2σ) between parentheses; experimental errors: I_{tot}/I_{MD}, ± 7%; estimated relative errors: n^3, ±10%; τ_{obs}, ± 2%; Q^{L}_{Ln}, ± 10%; τ_{rad}, ± 12%; Q^{Eu}_{Eu}, ± 12%; η_{sens}, ± 16%. [b] Calculated using eqs 2 and 3, n taken equal to 1.5 for solid samples and 1.4242 for solution in CH_2Cl_2. [c] From ref 52.

the $^5D_0$ level increases 3.2 fold up to 0.70 ms, a typical value for ternary lanthanide β-diketonates. It is fairly temperature insensitive thus confirming that the ligands in $[Eu(hfa)_3(bpyO2)]$ form a protective coordination environment around the metal ions, minimizing nonradiative deactivations either vibrational or electronic in nature. Absolute luminescence quantum yields (Q^{L}_{Ln}) measured under ligand excitation reach 40% for solid state $[Eu(hfa)_3(bpyO2)]$ and 35% for its solution in CH_2Cl_2, that is, more than 15-times improvement compared with $[Eu(hfa)_3(H_2O)_2]$. Intrinsic quantum yields could not be measured directly because of the faint $^5D_0 \leftarrow {}^7F_0$ absorption band (Figure 4) and were thus estimated from the following equations:[51]

$$Q^{Eu}_{Eu} = \frac{\tau_{obs}}{\tau_{rad}} \tag{2a}$$

$$\frac{1}{\tau_{rad}} = A_{MD,0} \cdot n^3 \cdot \left(\frac{I_{tot}}{I_{MD}}\right) \tag{2b}$$

with $A_{MD,0}$ being a constant equal to 14.65 s^{-1} and (I_{tot}/I_{MD}) the ratio of the total integrated $^5D_0 \rightarrow {}^7F_J$ emission (taken here as J = 0−4) to the integrated intensity of the magnetic-dipole $^5D_0 \rightarrow {}^7F_1$ transition. The refractive index n for the solid sample was set to 1.5, a value commonly encountered for coordination compounds. In case of solution, n was taken equal to the one of the neat solvent CH_2Cl_2, 1.4242. Analysis of the data shows that Q^{Eu}_{Eu} increases 4.3 times, up to 82%, upon substitution of water molecules with bpyO2 in solid state $[Eu(hfa)_3(bpyO2)]$. The radiative lifetime of solid $[Eu(hfa)_3(bpyO2)]$ is equal to 0.85 ms, that is, shorter by 25% compared to the initial hydrate despite a similar chemical environment (LnO_8). As expected from the refractive index dependence of τ_{rad} (eq 2b), this lifetime increases in CH_2Cl_2 solution to 0.94 ms: the ratio (0.85/0.94) = 0.90 being indeed consistent with the refractive index correction ($1.4242^3/1.5^3$) = 0.86. The intrinsic quantum yield for the CH_2Cl_2 solution is 30% smaller compared to the solid state sample; one-third of this decrease is attributable to the longer radiative lifetime only, so that the additional decrease points to collisional deactivation through solvent molecules.

Finally, the sensitization efficiency (η_{sens}) was estimated from

$$\eta_{sens} = \left(\frac{Q^{L}_{Eu}}{Q^{Eu}_{Eu}}\right) \tag{3}$$

and found to be approximately equal, within experimental errors, for solid $[Eu(hfa)_3(bpyO2)]$ and its solution in CH_2Cl_2, 49 and 55%, respectively. These values are ~4-fold larger than for $[Eu(hfa)_3(H_2O)_2]$. They remain, however, modest, reflecting energy losses occurring within the organic ligands before or during the transfer process onto the metal ion.

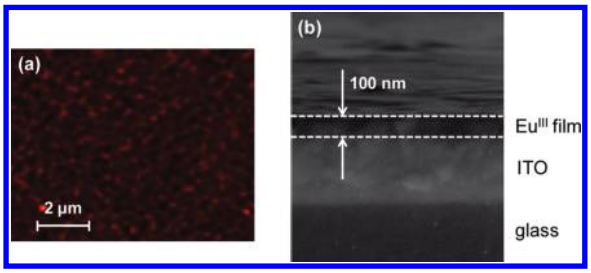

Figure 6. (a) AFM image of the surface and (b) SEM image of the chip of thin film obtained by thermal evaporation of $[Eu(hfa)_3(bpyO2)]$.

On the other hand the ancillary ligand bpyO2 has a detrimental effect on the luminescence of the Tb^{III} complex: while the initial hydrate $[Tb(hfa)_3(H_2O)_2]$ possesses sizable quantum efficiency, 27%, the replacement of water with bpyO2 results in almost complete quenching of Tb^{III} emission, with quantum yield down to 0.75% and a shortening of the $^5D_4$ luminescence lifetime from 0.53 ms to a value shorter than the measurable limit. This result arises from the close energetic proximity of the bpyO2 triplet state and the $^5D_4$ level. Efficient temperature-dependent back-transfer occurs, which is reduced at 77 K, as indicated by the restored value of the $^5D_4$ lifetime: 0.69 ms, close to the value for the bis(hydrate).

Thin Films. Thin films of $[Eu(hfa)_3(bpyO2)]$ with thickness of ≈100 nm were obtained by thermal evaporation in high vacuum (Figure 6). Their surface morphology was investigated to determine the average roughness. The results show that the $[Eu(hfa)_3(bpyO2)]$ thin film is smooth with root-mean-square roughness (rms) of ≈3 nm, although it has some pinholes.

The thin film exhibits bright red luminescence under UV excitation due to characteristic f-f transitions of the Eu^{III} ion. Relative integral intensities of hypersensitive $^5D_0 \rightarrow {}^7F_2$ and $^5D_0 \rightarrow {}^7F_4$ transitions decrease by 35 and 14%, respectively, in comparison with that of the initial bulk $[Eu(hfa)_3(bpyO2)]$ powder. The luminescence lifetime of a freshly prepared thin film is equal to 0.52(3) ms, which is shorter by 35 or 15% compared to that of the powder sample or of the solution in CH_2Cl_2, respectively (Table 3). After 2 months τ_{obs} of the thin film was remeasured and was found to be slightly larger, 0.60(3) ms, thus pointing to long-term stability of this material.

dx.doi.org/10.1021/ic200450x |Inorg. Chem. 2011, 50, 5137–5144

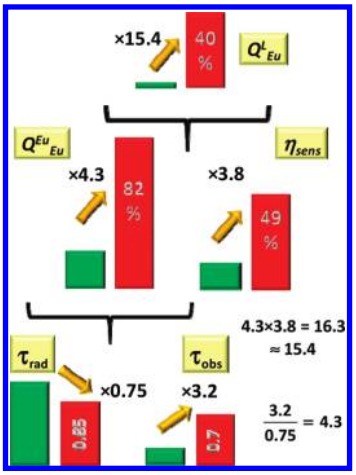

Figure 7. Role of bpyO2 in the sensitization of the luminescence of solid state $[Eu(hfa)_3(bpyO2)]$ (red rectangles) at room temperature; green rectangles pertain to $[Eu(hfa)_3(H_2O)_2]$; lifetimes are given in ms (lower panel).

CONCLUSION

Altogether, the photophysical data reported here confirm the important role played by the ancillary ligand in $[Eu(hfa)_3(bpyO2)]$ in (i) increasing the energy transfer efficiency, (ii) eliminating nonradiative deactivation pathways, and (iii) reducing the radiative lifetime. This is exemplified in Figure 7, which details the variation of the photophysical parameters for solid state samples in going from the bis(hydrate) to the ternary complex.

The introduction of $bpyO_2$ in the inner coordination sphere results in a 3.8-fold increase in the overall sensitization efficiency; assuming that the role of hfa^- remains the same in both compounds, this means that approximately 3/4 of the energy transfer is due to the ancillary ligand in the ternary complex. Removal of water molecules largely influences the observed lifetime which sustains a 3.2-fold increase because nonradiative deactivation through harmonics of O−H vibrations is suppressed. Interestingly, however, the intrinsic quantum yield increases more, 4.3 times, and this is due to a decrease in the radiative lifetime (−25%). The quantitative relationship between this parameter and the electronic structure of the complexes is still unclear,[29] and chelate designers usually do not consider radiative lifetime tuning in the tailoring of ligands with large sensitization efficiencies. It is nevertheless clear that increasing 4f-orbital mixing will decrease τ_{rad} and will have a beneficial influence on the intrinsic and overall quantum yields, as demonstrated here when water is replaced by the aromatic ancillary molecule bpyO2. A similar trend has been recently reported for one-dimensional coordination polymers $[Eu(hfa)_3(Q)]$ with various aromatic bidentate O-donors.[6] When Q = 1,4-dimethyltherephtalate, the sensitization efficiency is equal, within experimental errors, to the one reported here for the mononuclear ternary complex with bpyO2, but the overall quantum yield is ≈27% larger, a difference almost entirely due to a shorter radiative lifetime (−21%). It seems therefore important to give more attention to this parameter so as to have an additional handle to influence the construction of highly luminescent lanthanide complexes.

EXPERIMENTAL SECTION

General Methods, Instruments, and Reagents Used. Commercially available starting reagents were received from Merck or Aldrich and used as received. Lanthanide nitrate hydrates $Ln(NO_3)_3 \cdot xH_2O$ were obtained by treating the respective lanthanide oxides Ln_2O_3 (99.998%) or Tb_4O_7 (99.998%) with concentrated nitric acid, followed by evaporation of excess acid. $[Ln(hfa)_3(H_2O)_2]$ was synthesized according to the procedure described in the literature.[53] Elemental analyses (C, H, N) were performed on Vario Micro Cube (Elementar, Germany) by the Microanalytical Service of the Lomonosov Moscow State University. IR spectra were recorded on bulk samples in the range 4000−600 cm^{-1} with a Perkin-Elmer Spectrum One spectrometer equipped with a universal attenuated total reflection sampler. LDI-TOF mass spectra were run on an Autoflex II (Bruker Daltonics, Germany) using the electron-impact positive mode (accelerating voltage 19 kV) and a nitrogen laser (337 nm, impulse duration 1 ns). Assignment of the peaks was difficult because of heavy fragmentation of the molecules independent of the experimental conditions tried so that reliable data could only be obtained for the Eu^{III} derivative in view of its specific isotopic distribution. Thermogravimetric analysis was performed under nitrogen atmosphere on a Q-1500 thermal analyzer or in vacuum (10^{-2} Torr) on a ULVAC SINKU-RIKO TA-7000 analyzer at heating rates of 5 or 10 °C min^{-1}, respectively.

Emission and excitation spectra were measured with a Fluorolog FL3-22 spectrofluorimeter from Horiba-Jobin-Yvon Ltd. and corrected for the instrumental functions. Lifetimes were determined under ligand excitation and monitoring the $^5D_0 \rightarrow {}^7F_2$ (Eu^{III}) or $^5D_4 \rightarrow {}^7F_5$ (Tb^{III}) transitions using either a Fluorolog FL3-22 spectrofluorimeter or a home-built system with a nitrogen laser (λ_{ex} = 337 nm) and a boxcar averager system (model 162), including gated integrators (model 164) and wide-band preamplifier (model 115) from EG&G Princeton applied research. Luminescence decays were analyzed with Origin and proved to be single-exponential functions in all cases. Quantum yields were determined with the Fluorolog FL3-22 spectrofluorimeter at room temperature under excitation into ligand states according to an absolute method[54] using a home-modified integration sphere.[55] Each sample was measured several times under slightly different experimental conditions. The estimated error for quantum yields is ±10%.

Synthesis. *$[Ln(hfa)_3(bpyO2)]$ (Ln^{III} = Eu, Gd, Tb, Lu)* were synthesized according to a general procedure: equimolar amounts of $[Ln(hfa)_3(H_2O)_2]$ and bpyO2 were refluxed in benzene or toluene for 2 h, then the solution was cooled and further evaporation of the solvent yielded colorless precipitates which were isolated by decantation and dried in air. Yield: 95−100%.

$[Eu(hfa)_3(bpyO2)]$, $C_{25}H_{11}F_{18}O_8N_2Eu$ (960.95): calcd C 31.24, H 1.15, N 2.92; found C 31.32, H 1.18, N 2.97. IR data: $\tilde{\nu}$ = 3141 vw; 3106 vw; 2989 vw; 2872vw; 2902 vw; 2166 vw; 2052 vw; 2016 vw; 1730 vw; 1650 s; 1610 w; 1556 m; 1529 m; 1500 m; 1480 s; 1449 w; 1430 m; 1347 w; 1321 w; 1251 s; 1195 s; 1133 vs; 1096 s; 1035 m; 950 w; 853 m; 838 m; 797 s; 770 s; 740 m; 721 m; 684 w; 659 s cm^{-1}. LDI-TOF MS (EI^+): 549, $[Eu(hfa)_2(bpyO2)-C(O)CF_3-F-(C_5H_4N)+4H]^+$ (7%); 566, $[Eu(hfa)_2(bpyO2)-C(O)CF_3-(C_5H_4N)+4H]^+$ (8%); 601, $[Eu(hfa)_2(bpyO2)F_2-2C(O)CF_3+2H]^+$ (8%); 756, $[Eu(hfa)_2(bpyO2)+H]^+$ (100%); 790, $[Eu(hfa)_3(bpyO2)F-2C(O)CF_3+3H]^+$ (35%); 849, $[Eu(hfa)_2(bpyO2)_2-(C_5H_4N)]^+$ (13%); 941, $[Eu(hfa)_3(bpyO2)-F]^+$ (83%).

$[Gd(hfa)_3(bpyO2)]$, $C_{25}H_{11}F_{18}O_8N_2Gd$ (965.95): calcd C 31.08, H 1.15, N 2.90; found C 31.16, H 1.13, N 2.98. IR data: $\tilde{\nu}$ = 3142 vw; 3106 vw; 2160 vw; 2051 vw; 2035 vw; 1976 vw; 1650 s; 1610 w; 1557 m; 1530 m; 1496 m; 1480 m; 1449 w; 1430 m; 1349 w; 1321 vw; 1252 s; 1196 s; 1134 vs; 1097 s; 1034 m; 950 w; 853 m; 797 s; 770 s; 741 m; 720 m; 660 s cm^{-1}.

$[Tb(hfa)_3(bpyO2)]$, $C_{25}H_{11}F_{18}O_8N_2Tb$ (967.95): calcd C 31.02, H 1.14, N 2.89; found C 30.96, H 1.17, N 2.96. IR data: $\tilde{\nu}$ = 3141 vw; 2980 vw; 2902 vw; 2324 vw; 2174 vw; 2164 vw; 1650 s; 1557 m; 1530 m; 1497 m; 1480 m; 1449 w; 1429 m; 1349 w; 1328 w; 1252 s; 1197 s; 1136 vs; 1098 s; 1034 m; 951 w; 853 m; 839 m;798 s; 770 s; 741 m; 719 w; 660 s cm^{-1}.

Table 4. Crystal Data and Structure Refinement

	$[Eu(hfa)_3(bpyO2)]\cdot 0.5\ C_6H_6$ (**1**)
formula unit	$C_{25}H_{11}EuF_{18}N_2O_8\cdot 0.5C_6H_6$
molecular weight	1000.37
crystal system	monoclinic
space group	$P2_1/n$
a/Å	12.7679(17)
b/Å	13.9944(19)
c/Å	19.567(3)
α/deg	90.00
β/deg	96.837(5)
γ/deg	90.00
V/Å^3	3471.4(8)
Z	4
$\rho_{calc.}$/g·cm^{-3}	1.914
T/K	100(2)
μ/cm^{-1}	19.54
total reflections	9063
observed reflections [$I > 2\sigma(I)$]	7585
parameters refined	534
R_1 [$I > 2\sigma(I)$]	0.0294
ωR_2 [$I > 2\sigma(I)$]	0.0712

$[Lu(hfa)_3(bpyO2)]$, $C_{25}H_{11}F_{18}O_8N_2Lu$ (983.95): calcd C 30.51, H 1.12, N 2.85; found C 30.68, H 1.23, N 2.93. IR data: $\tilde{\nu}$ = 3144 vw; 3063 vw; 2323 vw; 2189 vw; 2027 vw; 1672 vw; 1653 s; 1597 w; 1557 m; 1529 m; 1509 m; 1479 m; 1450 w; 1432 m; 1350 w; 1325 vw; 1302 vw; 1250 s; 1215 s; 1204 s; 1192 s; 1163 s; 1133 vs; 1100 s; 1035 m; 1002 w; 992 w; 153 w; 886 w; 855 m; 840 m; 797 s; 773 s; 742 m; 720 w; 686 m; 661 s cm^{-1}.

[Lu(NO$_3$)$_3$(bpyO2)] was synthesized by mixing of ethanol solutions of $Lu(NO_3)_3\cdot 4H_2O$ with bpyO2 in molar ratio 1:1 under heating at 50 °C. After the white precipitate was formed, it was filtered off and dried under vacuum at 60−70 °C during 30 min. Yield: 90%.

$[Lu(NO_3)_3(bpyO2)]$, $C_{10}H_8LuN_5O_{11}$ (549.16): calcd C 21.87, H 1.47, N 12.75, Lu 31.9; found C 21.71, H 1.55, N 12.89, Lu 31.8. IR data: $\tilde{\nu}$ = 3095 m; 2424w; 2324w; 2165w; 2107vw; 2020vw; 1988w; 1972w; 1639 m; 1504 m; 1475s; 1445 m; 1425s; 1381w; 1307s; 1294s; 1258s; 1230s; 1213s; 1158 m; 1122 m; 1104 m; 1033s; 958w; 850s; 836s; 815 m; 770s; 750s; 734 m; 718 m cm^{-1}.

X-ray Single Crystal Analysis. Single crystals of **1** were obtained by slow evaporation of benzene solution of $[Eu(hfa)_3(bpyO2)]$ after 1 week. Diffraction data were collected on a Bruker SMART APEX II CCD diffractometer (MoK_α λ = 0.71072 Å) at 100 K. Empirical absorption correction was applied using Bruker SADABS program package.[56] The structure was solved by direct methods and refined by the full-matrix least-squares technique against F^2 in the anisotropic-isotropic approximation. Analysis of electron density synthesis have revealed that two CF_3 groups are disordered by two positions with occupancies 0.732(3), 0.268(3) and 0.787(5), 0.213(5). The hydrogen atoms were located from the Fourier density synthesis and refined with the riding model. All calculations were performed with the SHELXTL software package.[57] Crystallographic data and some details of data collection and structure refinement are listed in Table 4. Crystallographic data of **1** in CIF format (CCDC no. 815831) can be obtained, upon request, from the Director, Cambridge Crystallographic Data Centre, 12 Union Road, Cambridge CB2 1EZ, U.K.

Thin Films. Thin films of $[Eu(hfa)_3(bpyO2)]$ were deposited on 1−2 cm^2 glass/ITO substrates by thermal evaporation in vacuum chamber Univex-300 from Leybold Heraeus ($P < 3 \times 10^{-5}$ Torr) equipped with a quartz indicator (Inficon IC-6000) for thickness control. Morphology of the thin films was studied by scanning electron microscopy (SEM) on a Supra 50 VP (LEO) or on NT-MDT NTEGRA Aura in semicontact mode of atomic force microscopy (AFM). Data treatment was performed using the FemtoScan program package. To estimate the root-mean-square roughness, at least two samples were scanned at six different points or areas. Thickness of thin films was evaluated by SEM on chips and was found to be ≈100 nm.

■ ASSOCIATED CONTENT

Supporting Information. Crystallographic data of the $[Eu(hfa)_3(bpyO2)]\cdot 0.5\ C_6H_6$ (**1**) (CCDC no. 815831) in CIF format. This material is available free of charge via the Internet at http://pubs.acs.org.

■ AUTHOR INFORMATION

Corresponding Author
*E-mail: svetlana.eliseeva@chem.kuleuven.be.

■ ACKNOWLEDGMENT

Financial support from the Russian Foundation of Basic Research (Grant 09-03-00850-a) is acknowledged. The authors are grateful to Dr. Alexey V. Garshev (MSU, Russia), Dmitry M. Tsymbarenko (MSU, Russia), and Andrey A. Vaschenko (Lebedev Physical Institute, Russia) for their help with SEM, AFM measurements, and thin film preparation. S.E. and J.C.B. thank the Swiss National Science Foundation for financial support (Grant 200020_119866/1).

■ REFERENCES

(1) Binnemans, K. In *Handbook on the Physics and Chemistry of Rare Earths*; Gschneidner, K. A., Jr., Bünzli, J.-C. G., Pecharsky, V. K., Eds.; Elsevier Science B.V.: Amsterdam, The Netherlands, 2005; Vol. 35, Chapter 225, pp 107−272.
(2) Filipescu, N.; Mushrush, G. W. *Nature* **1966**, *211*, 960.
(3) Malandrino, G.; Fragalà, I. L. *Coord. Chem. Rev.* **2006**, *250*, 1605.
(4) Yin, K.; Xu, H.; Zhong, G. Y.; Ni, G.; Huang, W. *Appl. Phys. A: Mat. Sci. Process.* **2009**, *95*, 595.
(5) Stanley, J. M.; Zhu, X.; Yang, X.; Holliday, B. J. *Inorg. Chem.* **2010**, *49*, 2035.
(6) Eliseeva, S. V.; Pleshkov, D. N.; Lyssenko, K. A.; Lepnev, L. S.; Bünzli, J.-C. G.; Kuzmina, N. P. *Inorg. Chem.* **2010**, *49*, 9300.
(7) Eliseeva, S. V.; Kotova, O. V.; Gumy, F.; Semenov, V. V.; Kessler, V. G.; Lepnev, L.; Bünzli, J.-C. G.; Kuzmina, N. *J. Phys. Chem. A* **2008**, *112*, 3614.
(8) Hasegawa, Y.; Nakagawa, T.; Kawai, T. *Coord. Chem. Rev.* **2010**, *254*, 2643.
(9) Wang, Y.; Wang, L.; Li, H.; Liu, P.; Qin, D.; Liu, B.; Zhang, W.; Deng, R.; Zhang, H. *J. Solid State Chem.* **2008**, *181*, 562.
(10) Mudring, A.-V. *Eur. J. Inorg. Chem.* **2009**, 2769.
(11) Bruno, S. M.; Ferreira, R. A. S.; Almeida Paz, F. A.; Carlos, L. D.; Pillinger, M.; Ribeiro-Claro, P.; Goncalves, I. S. *Inorg. Chem.* **2009**, *48*, 4882.
(12) Li, H. R.; Cheng, W. J.; Wang, Y.; Liu, B. Y.; Zhang, W. J.; Zhang, H. J. *Chem.—Eur. J.* **2010**, *16*, 2125.
(13) Dumke, J. C.; El-Zahab, B.; Challa, S.; Das, S.; Chandler, L.; Tolocka, M.; Hayes, D. J.; Warner, I. M. *Langmuir* **2010**, *26*, 15599.
(14) Hasegawa, J.; Hieda, R.; Nakagawa, T.; Kawai, T. *Helv. Chim. Acta* **2009**, *92*, 2238.
(15) Wang, Q. M.; Ogawa, K.; Toma, K.; Tamiaki, H. *J. Photochem. Photobiol., A* **2009**, *201*, 87.

(16) Dong, H. T.; Liu, Y.; Wang, D. D.; Zhang, W. Z.; Ye, Z. Q.; Wang, G. L.; Yuan, J. L. *Nanotechnology* **2010**, *21*, 395504.
(17) He, P.; Wang, H. H.; Liu, S. G.; Hu, W.; Shi, J. X.; Wang, G.; Gong, M. L. *J. Electrochem. Soc.* **2009**, *156*, E46–E49.
(18) Eliseeva, S. V.; Bünzli, J.-C. G. *New J. Chem.* **2011**, *35*, published on the web February 2, 2011, DOI: 10.1039/c0nj00969e.
(19) Katkova, M. A.; Bochkarev, M. N. *Dalton Trans* **2010**, *39*, 6599.
(20) Balamurugan, A.; Reddy, M. L. P.; Jayakannan, M. *J. Phys. Chem. B* **2009**, *113*, 14128.
(21) Law, G. L.; Wong, K. L.; Tam, H. L.; Cheah, K. W.; Wong, W. T. *Inorg. Chem.* **2009**, *48*, 10492.
(22) Valore, A.; Cariati, E.; Righetto, S.; Roberto, D.; Tessore, F.; Ugo, R.; Fragala, I. L.; Fragala, M. E.; Malandrino, G.; De Angelis, F.; Belpassi, L.; Ledoux-Rak, I.; Thi, K. H.; Zyss, J. *J. Am. Chem. Soc.* **2010**, *132*, 4966.
(23) Pihlasalo, S.; Hara, M.; Hanninen, P.; Slotte, J. P.; Peltonen, J.; Harma, H. *Anal. Biochem.* **2009**, *384*, 231.
(24) Jiang, L. N.; Wu, J.; Wang, G. L.; Ye, Z. Q.; Zhang, W. Z.; Jin, D. Y.; Yuan, J. L.; Piper, J. *Anal. Chem.* **2010**, *82*, 2529.
(25) Bünzli, J.-C. G. *Chem. Rev.* **2010**, *110*, 2729.
(26) Tsvirko, M. P.; Meshkova, S. B.; Venchikov, V. Y.; Topilova, Z. M.; Bol'shoi, D. V. *Opt. Spectrosc. (Engl. Transl.)* **2001**, *90*, 669.
(27) Comby, S.; Bünzli, J.-C. G. In *Handbook on the Physics and Chemistry of Rare Earths*; Gschneidner, K. A., Jr., Bünzli, J.-C. G., Pecharsky, V. K., Eds.; Elsevier Science B. V.: Amsterdam, The Netherlands, 2007; Vol. 37, Chapter 235, pp 217−470.
(28) Malta, O. L.; Brito, H. F.; Menezes, J. F. S.; Gonçalves e Silva, F. R.; Donega, C. D.; Alves, S. *Chem. Phys. Lett.* **1998**, *282*, 233.
(29) Bünzli, J.-C. G.; Chauvin, A.-S.; Kim, H. K.; Deiters, E.; Eliseeva, S. V. *Coord. Chem. Rev.* **2010**, *254*, 2623.
(30) Biju, S.; Reddy, M. L. P.; Cowley, A. H.; Vasudevan, K. V. *Cryst. Growth Des.* **2009**, *9*, 3562.
(31) Divya, V.; Freire, R. O.; Reddy, M. L. P. *Dalton Trans.* **2011**, *40*, 3257.
(32) Huskowska, E.; Turowska-Tyrk, I.; Legendziewicz, J.; Riehl, J. P. *New J. Chem.* **2002**, *26*, 1461.
(33) Malta, O. L.; Legendziewicz, J.; Huskowska, E.; Turowska-Tyrk, I.; Albuquerque, R. Q.; Donega, C. D.; Silva, F. R. G. E. *J. Alloys Compd.* **2001**, *323*, 654.
(34) Ulrich, G.; Hissler, M.; Ziessel, R. F.; Manet, I.; Sarti, G.; Sabbatini, N. *New J. Chem.* **1997**, *21*, 147.
(35) Prodi, L.; Pivari, S.; Bolletta, F.; Hissler, M.; Ziessel, R. *Eur. J. Inorg. Chem.* **1998**, 1959.
(36) Martynenko, L. I.; Kuzmina, N. P.; Grigorev, A. N. *Zh. Neorg. Khim.* **1996**, *41*, 976.
(37) Martynenko, L. I.; Kuzmina, N. P.; Grigorev, A. N. *Zh. Neorg. Khim.* **1998**, *43*, 1131.
(38) De Silva, C. R.; Maeyer, J. R.; Wang, R. Y.; Nichol, G. S.; Zheng, Z. *Inorg. Chim. Acta* **2007**, *360*, 3543.
(39) Tedmann, O. M.; Madan, S. K.; Zavalij, P. Y.; Oliver, S. R. J. *Inorg. Chim. Acta* **2007**, *360*, 3408.
(40) Kanno, H.; Omotera, Y.; Iijima, K. *Acta Crystallogr., Sect. C* **1998**, *54*, 149.
(41) Puntus, L. N.; Lyssenko, K. A.; Pekareva, I.; Bünzli, J.-C. G. *J. Phys. Chem. B* **2009**, *113*, 9265.
(42) Brown, I. D. *Chem. Rev.* **2009**, *109*, 6858.
(43) Trzesowska, A.; Kruszynski, R.; Bartczak, T. J. *Acta Crystallogr., Sect. B* **2004**, *60*, 174.
(44) Xu, J. D.; Radkov, E.; Ziegler, M.; Raymond, K. N. *Inorg. Chem.* **2000**, *39*, 4156.
(45) Porai-Koshits, M. A.; Aslanov, L. A. *Zh. Strukt. Khim. (Engl. Transl.)* **1972**, *13*, 244.
(46) Eliseeva, S. V.; Bünzli, J.-C. G. *Chem. Soc. Rev.* **2010**, *39*, 189.
(47) Tobita, S.; Arakawa, M.; Tanaka, I. *J. Phys. Chem.* **1985**, *89*, 5649.
(48) Tobita, S.; Arakawa, M.; Tanaka, I. *J. Phys. Chem.* **1984**, *88*, 2697.
(49) Bünzli, J.-C. G.; Eliseeva, S. V. In *Springer Series on Fluorescence. Lanthanide Luminescence: Photophysical, Analytical and Biological Aspects*; Hänninen, P., Härmä, H., Eds.; Springer Verlag: Berlin, Germany, 2010; Vol. 8, Chapter published on line July 15, DOI: 10.1007/4243_2010_3.
(50) Bünzli, J.-C. G. In *Lanthanide Probes in Life, Chemical and Earth Sciences. Theory and Practice*; Bünzli, J.-C. G., Choppin, G. R., Eds.; Elsevier Science Publ. B.V.: Amsterdam, The Netherlands, 1989, Chapter 7; pp 219−293.
(51) Werts, M. H. V.; Jukes, R. T. F.; Verhoeven, J. W. *Phys. Chem. Chem. Phys.* **2002**, *4*, 1542.
(52) Eliseeva, S. V.; Ryazanov, M.; Gumy, F.; Troyanov, S. I.; Lepnev, L. S.; Bünzli, J.-C. G.; Kuzmina, N. P. *Eur. J. Inorg. Chem.* **2006**, 4809.
(53) Richards, M. F.; Wagner, W. F.; Sands, D. E. *J. Inorg. Nucl. Chem.* **1968**, *30*, 1275.
(54) de Mello, J. C.; Wittmann, H. F.; Friend, R. H. *Adv. Mater.* **1997**, *9*, 230.
(55) Aebischer, A.; Gumy, F.; Bünzli, J.-C. G. *Phys. Chem. Chem. Phys.* **2009**, *11*, 1346.
(56) Sheldrick, G. M. *SADABS, Program for semiempirical absorption correction of area detector data*; University of Göttingen: Göttingen, Germany, 1996.
(57) *SHELXTL*, release 6.1.4; Bruker AXS Inc.: Madison, WI, 2003.